

# CONTRAST ENHANCEMENT BASED SINGLE IMAGE DEHAZING VIA TV- $\ell_1$ MINIMIZATION

Liang Li<sup>1,2</sup>, Wei Feng<sup>1,2</sup>, Jiawan Zhang<sup>3,\*</sup>

<sup>1</sup> School of Computer Science and Technology, Tianjin University, Tianjin, China

<sup>2</sup> Tianjin Key Laboratory of Cognitive Computing and Application, Tianjin University, Tianjin, China

<sup>3</sup> School of Computer Software, Tianjin University, Tianjin, China

{liangli, wfeng, jwzhang}@tju.edu.cn

## ABSTRACT

In this paper, we propose a general algorithm to removing haze from single images using total variation minimization. Our approach stems from two simple yet fundamental observations about haze-free images and the haze itself. First, clear-day images usually have stronger contrast than images plagued by bad weather; and second, the variations in natural atmospheric veil, which highly depends on the depth of objects, always tend to be smooth. Integrating these two criteria together leads to a new effective dehazing model, which encourages the gradient  $\ell_1$  sparsity of atmospheric veil and implicitly maximizes the global contrast of haze-free image in the meanwhile. We also show that the proposed dehazing model can be efficiently solved using the TV- $\ell_1$  minimization. Compared to alternative state-of-the-art methods, our approach is physically plausible and works well for all types of hazy situations. Comparative study and quantitative evaluation on both synthetic and natural images validate the superior performance and the generality of our approach.

*Index Terms*— Image dehazing, visibility restoration, contrast enhancement, total variation minimization

## 1. INTRODUCTION

The photographs we get in our daily life are very easy to be plagued by various aerosols suspended in the air, such as dust, mist, and/or fumes. Due to the existing aerosols, the rays reflected by the surfaces of objects are not only attenuated but also blended with the airlight, before they reach the observers. This inevitably results in poor visibility and contrast lost in the image. As a result, the quality of photographs taken in hazy scenes are seriously degraded.

The goal of dehazing is to recover color, visibility and details of the scene from hazy images. There are many real-world circumstances, where accurate dehazing results are

highly required. In computer vision, most existing applications assume that the radiance from a scene point to observer is not altered by the airlight and intermediate medium. However, this assumption is not practical in hazy scenes, because the light energy radiating from scene points is heavily scattered by the atmosphere. Therefore, the performance of most computer vision applications may fail or significantly degraded in bad weather conditions. In consumer photography, the images will be annoying with the presence of fog that may severely lower the contrast. In aerial photography and remote sensing, the photos are much easier to be affected by aerosols. Even in clear days, the rays reflected by the ground will be scattered heavily by passing through the earth's atmosphere, which will degrade the image quality.

Recovering the visibility of hazy images is actually to restore the contrast. However, since the contrast lost caused by haze is depth dependent, classical techniques, such as histogram equalization, histogram specification and the recently proposed contrast correction method [1], can not be directly applied to hazy images, due to the lack of plausible physical foundations. In recent years, several successful contrast maximization methods specifically designed for dehazing have been proposed [2, 3, 4]. All of them are proven to be effective for some particular types of haze situations. According to [5], there are four different types of fog in total – that is, uniform fog, heterogeneous extinction coefficient fog, heterogeneous luminance fog, and heterogeneous both extinction coefficient and luminance fog. Many state-of-the-art haze removal methods for single images assumes the fog is uniform. Few of them quantitatively work well for different types of fog situations. In fact, how to uniformly remove all four types of fogs from single images is still an open problem.

In this paper we present a general approach to removing haze from single hazy images. We integrate two general criteria about the haze-free image and the atmospheric veil, i.e. maximizing the global contrast of haze-free image and minimizing the gradient  $\ell_1$  norm of atmospheric veil at the same time, to achieve the purpose of haze removal. We show that this problem can be effectively solved with the TV- $\ell_1$  [6] min-

\* is the corresponding author. This work is supported by NSFC (61100121, 61272266), and the National Science and Technology Support Project (2013BAK01B00, 2013BAK01B01, 2013BAK01B05 and 2013BAH62F02).

imization framework [6]. Since our approach is physically plausible and makes no further assumption about the haze model, it is applicable to and works well for all four types of fog situations, including the challenging case with heterogeneous extinction coefficient and luminance. We compare the proposed approach with several state-of-the-art methods, based on both benchmark synthetic images [7] and natural images. Experimental results validate the superiority of our method in restoration quality and generality.

The contribution of this paper lies in 2 aspects: a) We explicitly analyze that to maximize the global contrast of the haze-free image is equivalent to solve a minimizing problem and we solve this problem in TV- $\ell_1$  framework. b) We compare our result to state-of-the-art ones both qualitatively and quantitatively and the results show our algorithm can work well on both homogeneous and heterogeneous fog.

## 2. RELATED WORK

From an application point of view, dehazing algorithms are very useful in many fields. In remote sensing systems, the quality of sensing is heavily dependent on the weather. In [8], Zhang et al. removes the haze effect in sensing by assuming a uniform haze layer across the image. Haze effect also affects the safety of driving a vehicle. For the camera-based Advanced Driver Assistance System (ADAS), Tarel et al. [9] proposes an automatic fog detection and restoration algorithm in which the onboard camera parameters are leveraged. Regarding the large part of a road image is planar, visibility enhancement dedicated to planar surface was first proposed in [10]. In [5], another algorithm based on the planar assumption is introduced.

Dehazing from a single image is an challenge problem. Early approaches to restore visibility of hazy images focused on achieving the image decomposition with additional information. In [11], the polarized haze effect are removed given two photographs taken under different polarization state. In [12], user interactions is involved to dehaze. Recently, Schaul et al. proposes an algorithm [13] to restore the visibility based on near-infrared (NIR) information and it achieves good results. Kopf et al. [14] utilizes the 3D model of a city to restore the image. For this kind of algorithms, due to more information is utilized, the results is generally impressive.

In the context of computational photography, there is a great progress in single image dehazing [2, 15, 16, 17]. Relying on one or two reasonable assumption(s), the input for the algorithm is a single image. Fattal [15] assumed that the transmission and the surface shading are locally uncorrelated. He first inferred the transmission in the area affected by thin fog and then propagate the transmission to dense fog area. This approach is physically based and achieves good result. However, it fails when all pixels on the image are affected by dense fog. Tan [2] restores the visibility by locally maximizing contrast of the results. Since the contrast is maximize,

the results seems to be too saturated. He [18] proposed Dark Channel Prior to solve the single image dehazing problem. It extracts a coarse level transmission map and then refines it using *soft matting*. In He's latter work [19], he substitute the soft matting with *guided filter* which is more computational efficient. Tarel [4] proposed a more fast dehazing algorithm, of which the complexity is linear to the size of input image. *Sparse prior* is also used for dehazing [20].

Most of the dehazing algorithms assume the haze in the scene is homogeneous. The work on removing heterogeneous haze is relatively small. In [7] Tarel first proposes an algorithm working for both homogeneous and heterogeneous haze.

Among all these dehazing algorithms, it is difficult to tell which one is better than the other since there is a lack of ground truth data. In practice, to obtain a pair of images with and without fog is a hard work since it requires to check that the illumination conditions are the same into the scene with and without fog. To our best knowledge, there are mainly two quantitative measurements for the restore image. One is described in [21], the *mean visible edge ratio* can reflects the quality of the restored image to some extent. The other one is averaged *absolute difference* which is used in [5]. Tarel et al. [5] have already built some synthetic scenes with ground truth for evaluation purpose.

## 3. OUR ALGORITHM

The model widely used [4, 15, 18, 20] in computer graphics and computer vision to describe the formation of the hazy image is given by the Koschmieder's law:

$$\mathbf{I}(\mathbf{x}) = \mathbf{J}(\mathbf{x})e^{-kd(\mathbf{x})} + \left(1 - e^{-kd(\mathbf{x})}\right)\mathbf{L}_\infty, \quad (1)$$

where  $\mathbf{I}(\mathbf{x})$  is the hazy image,  $\mathbf{J}(\mathbf{x})$  is the haze-free image,  $k$  is the extinction coefficient of the haze,  $\mathbf{L}_\infty$  is the atmosphere color and  $d(\mathbf{x})$  denotes the distance of the object at pixel  $\mathbf{x} = (x, y)$ . For homogeneous haze, both  $\mathbf{L}_\infty$  and  $k$  are global constants over the whole image; for heterogeneous haze,  $\mathbf{L}_\infty$  and  $k$  may vary locally.

The addend and the augend in Eq. (1) describe two mechanisms of the fog: *direct attenuation* and airlight. Schechner's work [11] describes the two mechanisms in detail.

### 3.1. Initialization of atmospheric veil

With the concept *atmospheric veil* (or airlight map)  $\mathbf{V}(\mathbf{x}) = \mathbf{L}_\infty(1 - e^{-kd(\mathbf{x})})$  introduced by Tarel's work [4], Eq. (1) can be rewritten as,

$$\mathbf{I}(\mathbf{x}) = \mathbf{J}(\mathbf{x}) \left(1 - \frac{\mathbf{V}(\mathbf{x})}{\mathbf{L}_\infty}\right) + \mathbf{V}(\mathbf{x}). \quad (2)$$

As suggested by [4], white balance is performed on the hazy image before the visibility restoration algorithm. Once the white balance is correctly performed, the color of the sky  $\mathbf{L}_\infty$

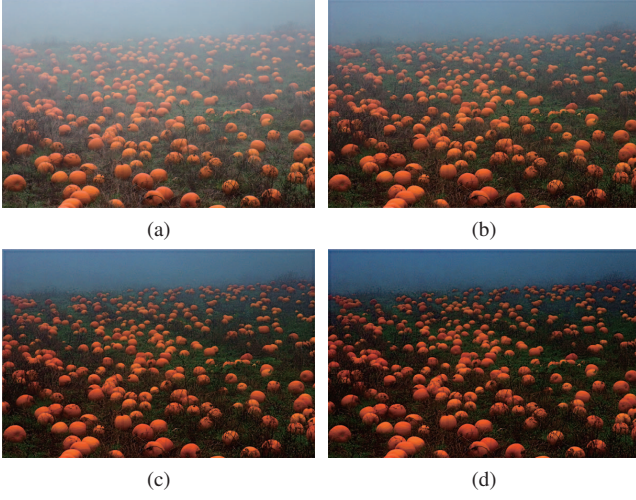


**Fig. 1.** The effect of  $\beta$  in Eq. (5). (a) The input hazy image. (b)-(d) The dehazing results obtained by setting  $\beta = 0.6$ ,  $\beta = 0.8$ ,  $\beta = 0.95$  respectively.

can be set to pure white, i.e.  $[1, 1, 1]$ . Thus, the atmospheric veil will be the product of  $[1, 1, 1]$  and a scalar map  $V(\mathbf{x}) = 1 - e^{-k d(\mathbf{x})}$ . For convenience, we call both  $\mathbf{V}(\mathbf{x})$  and  $V(\mathbf{x})$  the atmospheric veil.

It is easy to see  $V(\mathbf{x}) \geq 0$  due to its physical property. To get the maximum value of  $V(\mathbf{x})$ , we take the minimal of each component in Eq. (2) and it can be rearranged as,

$$\min_{c \in \{r, g, b\}} (\mathbf{I}^c(\mathbf{x})) - \min_{c \in \{r, g, b\}} (\mathbf{J}^c(\mathbf{x})(1 - V(\mathbf{x}))) = V(\mathbf{x}). \quad (3)$$

Since  $\min_{c \in \{r, g, b\}} (\mathbf{J}^c(\mathbf{x})) \geq 0$  and  $1 - V(\mathbf{x}) \geq 0$ , then we get

$$0 \leq V(\mathbf{x}) \leq \min_{c \in \{r, g, b\}} (\mathbf{I}^c(\mathbf{x})). \quad (4)$$

So we can initialize the atmospheric veil as,

$$V_0(\mathbf{x}) = \beta \min_{c \in \{r, g, b\}} (\mathbf{I}^c(\mathbf{x})), \quad (5)$$

where  $0 < \beta < 1$  is a constant that relates with the density of the fog. For an image with dense fog,  $\beta$  should be large and otherwise small. On the other hand,  $\beta$  can also be regarded as a parameter controls the strength of the visibility restoration. See Figure 1 for an example. Equation (5) is applicable for color images and we obviously have  $V(\mathbf{x}) = \beta I(\mathbf{x})$  for a gray scale hazy image.

### 3.2. Atmospheric veil refinement

As described in [4], maximizing the contrast of resulting image is equivalent to maximizing  $V(\mathbf{x})$  assuming than  $V(\mathbf{x})$  is smooth most of the time,

$$\arg \max_{\mathbf{V}} \int_{\Omega} V(\mathbf{x}) - \alpha \phi(\|\nabla V\|^2) dx, \quad (6)$$

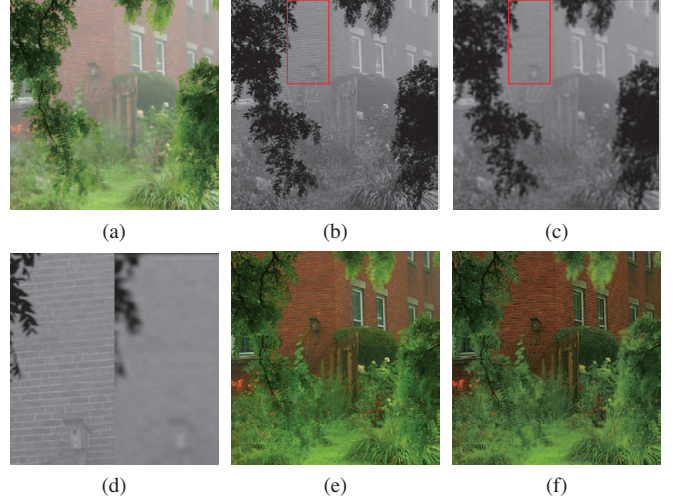


**Fig. 2.** Single image dehazing with TV- $\ell_1$  minimization. (a) The input image. (b) The initialization of atmospheric veil  $V_0(\mathbf{x})$ . (c) The final atmospheric veil  $V(\mathbf{x})$ . (d) Zoom in comparison. (e) Result using  $V_0(\mathbf{x})$ . (f) Result using  $V(\mathbf{x})$ . We can clearly see the improvements of (f) to (e).

where parameter  $\alpha$  controls the smoothness of the solution,  $\phi$  is an increasing concave function,  $\nabla V(\mathbf{x})$  is the derivatives of the atmospheric veil. Although Eq. (6) allows large jumps in  $V(\mathbf{x})$  (since  $\phi$  is concave), unfortunately, it is a non-convex optimization problem and thus the optimal solution may be hard to obtained.

Here, rather than maximizing a non-convex functional, we adapt *total variation minimization*, which was first proposed in image processing by Rudin, Osher and Fatemi (ROF model) [6], to pursuing the maximum of the atmospheric veil while allowing discontinuities along edges.

Formally, in our case, we minimize the following energy function to obtain the refined  $V(\mathbf{x})$ ,

$$\arg \min_{\mathbf{V}} \int_{\Omega} \|V_0 - V\|_2^2 + \alpha \|\nabla V(\mathbf{x})\|_1 dx, \quad (7)$$

where  $\|\cdot\|_n$  denotes  $\ell_n$  norm.  $\|\nabla V(\mathbf{x})\|_1$  in Eq. (7) is called total variation (TV) of  $V(\mathbf{x})$ .

Our model is physically plausible. In fact, we are pursuing such a  $V(\mathbf{x})$  that is close to  $V_0(\mathbf{x})$  and can only change dramatically along the edges. As illustrated in [22],  $\ell_1$  norm (total variation) can preserve the discontinuities in the original image well.

To minimize Eq. (7), Euler-Lagrange function can not be applied since the  $\ell_1$  norm is not differentiable. Here, we adapt the algorithm described by Chambolle [23] to get the solution. To illustrate the algorithm clearly, we give the discrete version of Eq. (7),

$$\arg \min_{\mathbf{V}} \|\mathbb{V}_0 - \mathbb{V}\|^2 + \alpha (\|\mathbb{D}_x \cdot \mathbb{V}\|_1 + \|\mathbb{D}_y \cdot \mathbb{V}\|_1), \quad (8)$$



where  $\mathbb{V}$  and  $\mathbb{V}_0$  are the vectorized version of  $V(\mathbf{x})$  and  $V_0(\mathbf{x})$  respectively,  $\mathbb{D}_x$  and  $\mathbb{D}_y$  denote the x- and y- derivative filters, i.e.  $\mathbb{D}_x \cdot \mathbb{V} = V * [-1, 0, 1]$ . Then the solution to Eq. (7) given by [23] is the following iterative process,

$$\begin{aligned} \mathbb{V}^{(i)} &= \mathbb{V}_0 + \alpha(\mathbb{M}^{(i)} + \mathbb{N}^{(i)}), \\ \mathbb{M}^{(i+1)} &= \frac{\mathbb{M}^{(i)} + (\tau/\alpha)\mathbb{D}_x\mathbb{V}^{(i)}}{\max\{1, |\mathbb{M}^{(i)} + (\tau/\alpha)\mathbb{D}_x\mathbb{V}^{(i)}|\}}, \\ \mathbb{N}^{(i+1)} &= \frac{\mathbb{N}^{(i)} + (\tau/\alpha)\mathbb{D}_y\mathbb{V}^{(i)}}{\max\{1, |\mathbb{N}^{(i)} + (\tau/\alpha)\mathbb{D}_y\mathbb{V}^{(i)}|\}}, \end{aligned} \quad (9)$$

where  $\tau > 0$  called ‘‘time-step’’ in [23] and should be  $\tau \leq 1/4$  to make the iteration converged,  $|\cdot|$  is the absolute value operator and is performed element-wise on a vector. As suggest by [23], we set  $0.24 \leq \tau \leq 0.249$  during our experiment and a good convergence can be obtained.

### 3.3. Visibility restoration

Once the atmospheric veil  $V(\mathbf{x})$  is estimated, each color component of the haze-free image  $\mathbf{J}(\mathbf{x})$  can be restored through Eq. (1). However, as illustrated in [18], the directly recovered intensity is prone to noise when  $V(\mathbf{x})$  is too close to 1. Therefore, we restrict the atmospheric veil  $V(\mathbf{x})$  to an upper bound  $V_b$ , which means a small certain amount of haze are preserved in very dense haze regions. The final intensity is recovered by,

$$\mathbf{J}(\mathbf{x}) = \frac{\mathbf{I}(\mathbf{x}) - \min(V(\mathbf{x}), V_b)}{1 - \min(V(\mathbf{x}), V_b)} \quad (10)$$

In our experiments, we set  $V_b = 0.9$  for all results.

## 4. RESULTS AND EVALUATIONS

We implement our algorithm with C++. Averagely, it takes about 1-2 seconds to get the final result for a  $600 \times 480$  hazy image on a PC with Intel Core™ i7-2600 processor and 8GB memory. As illustrated in [22], the process described by Eq. (9) usually converges after about 40-50 iterations. Hence, we set a fixed iteration number  $n = 70$  in our experiments. To evaluate the performance, we compare our approach with 5 state-of-the-art dehazing methods, i.e. Tarel [4], Tan [2], Fattal [15], He [18] and Kopf [14], on both benchmark synthetic images and natural scenes.

We first compare our approach with Tarel’s method [4] in removing homogeneous fog. As shown in Figure 3, for regions with high texture and sharp depth variance, e.g. the red-rectangle regions in Figure 3, Tarel’s method [4] could not produce satisfactory result, but our approach worked well. Besides homogeneous fog, our approach also works well for removing heterogeneous fogs. Figure 4 shows a challenging hazy case. We compare our approach with Tarel [4] and Fattal [15]. We note that all three methods could not fully remove the haze in the image (see the area marked by red rectangles),



**Fig. 3.** Comparison with Tarel’s method. (a) Restoration result by [4] for the hazy image Figure 2(a). (b) The result of our approach. Note that in the red rectangle region, due to sharp variations in depth, [4] can not process it well.

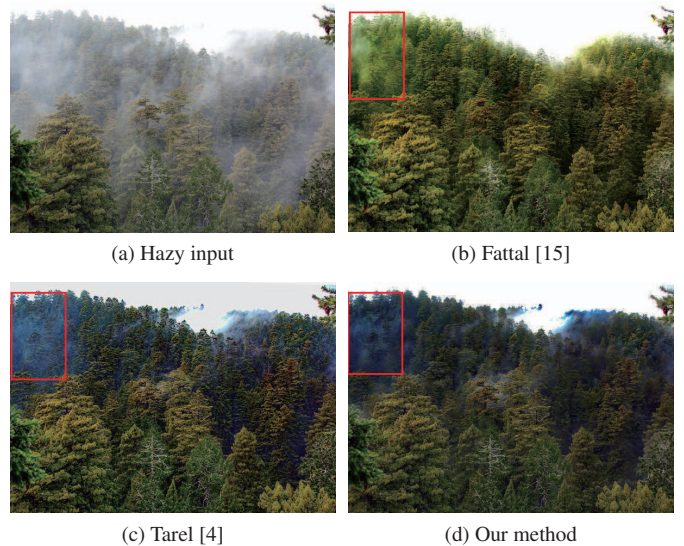


**Fig. 4.** The results of our approach to remove heterogeneous fog. Our result looks more natural than the other two, especially in the regions marked by red rectangles.

but our result looks more natural and of higher quality than the other two.

Figure 5 shows the results of our method compared with the other 4 state-of-the-art methods on single image dehazing. Note that, among the 4 methods, Kopf [14] utilizes the additional 3D model of the city for haze removal. We can see that, although the input of our approach is only a single image, our result is quite close to that of Kopf’s method and has the least tone deviation to the original image.

To quantitatively evaluate the performance of our approach, we utilized the synthetic image dataset built by Tarel et al. [5] for comparison. In this experiment, we also quantitatively evaluated 4 other methods, i.e. Fattal [15], Tan [2], He [18] and Tarel [4]. Following [5, 7], we calculated the average absolute difference between the restored image and

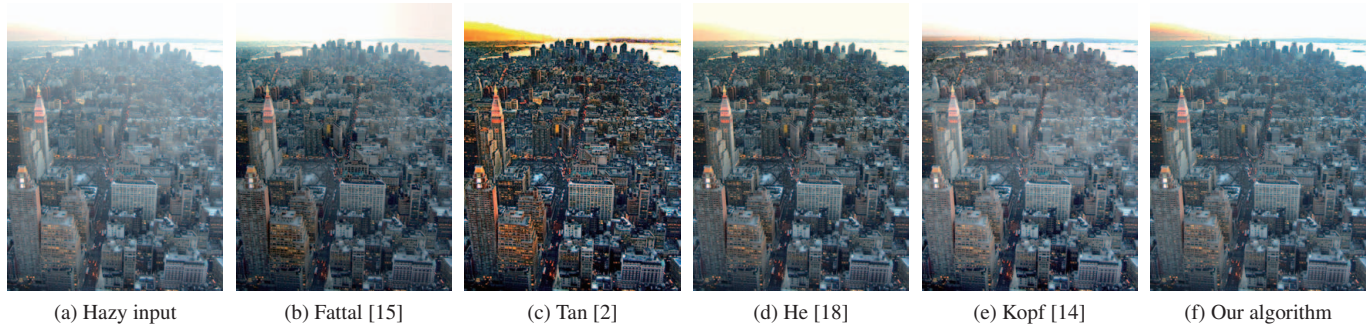


**Fig. 5.** Comparison to 4 state-of-the-art dehazing algorithms. (a) The original hazy image. (b)-(e) The results obtained by Tan [2], Fattal [15], He [18] and Kopf [14], respectively. (f) The result of our approach.

**Table 1.** The average *absolute difference* between restored image of 5 evaluated methods and the ground truth.

Algorithm	Uniform	Variable $k$	Vari. $L_\infty$	Vari. $k \& L_\infty$
Fattal [15]	$36.7 \pm 4.2$	$38.2 \pm 3.0$	$42.8 \pm 6.2$	$44.7 \pm 5.9$
Tan [2]	$45.2 \pm 4.0$	$44.0 \pm 3.4$	$42.9 \pm 12.8$	$49.1 \pm 4.4$
He [18]	$33.2 \pm 2.3$	$42.0 \pm 9.2$	$41.0 \pm 6.9$	$42.3 \pm 8.6$
Tarel [4]	$31.9 \pm 4.6$	<b><math>29.0 \pm 4.3</math></b>	$40.2 \pm 4.3$	$37.2 \pm 4.4$
Ours	<b><math>31.5 \pm 4.5</math></b>	$40.5 \pm 4.0$	<b><math>39.8 \pm 7.9</math></b>	<b><math>36.9 \pm 6.8</math></b>

the ground truth haze-free image. The comparative results are shown in Table 1, with the mean and standard deviation calculated over all 18 tested images. From Table 1, we can observe that our approach outperforms the other 4 state-of-the-art methods in handling all types of fog situations. For instance, our approach obtains the best performance for uniform fog, heterogeneous  $L_\infty$  fog, and the challenging heterogeneous  $k$  and  $L_\infty$  fog.

Figure 6 shows some results of our approach on the benchmark synthetic scenes generated by [5]. We select the scenes with both homogeneous and heterogeneous haze to demonstrate the effectiveness of our approach in handling various types of hazy scenes. Refer to the caption of Figure 6 for more details.

## 5. CONCLUSIONS AND FUTURE WORK

In this paper, we have proposed a new algorithm to remove haze from a single image using TV- $\ell_1$  minimization. TV- $\ell_1$  can preserve the large jumps in atmospheric veil and can also implicitly maximize the global contrast in the restored image. Moreover, our approach is physically plausible and relies no further assumption on the fog model. Experimental results show that the proposed approach works well for dealing with all four types of haze situations. The quantitative evaluation also demonstrates the general and superior performance of our approach over state-of-the-art single image dehazing methods. In the future, we plan to extend our model to handle large-scale atmosphere-color-like object based on segmentation and separate treatment. Besides, we plan to work

on superpixel grid [24] to gain more efficiency.

## 6. REFERENCES

- [1] J. Oakley and H. Bu, “Correction of simple contrast loss in color images,” *IEEE Trans. on Image Process.*, vol. 16, no. 2, pp. 511–522, 2007.
- [2] R. Tan, “Visibility in bad weather from a single image,” in *CVPR*, 2008, pp. 1–8.
- [3] J.-H. Kim, J.-Y. Sim, and C.-S. Kim, “Single image dehazing based on contrast enhancement,” in *ICASSP*, 2011.
- [4] J.-P. Tarel and N. Hautière, “Fast visibility restoration from a single color or gray level image,” in *ICCV*, 2009.
- [5] N. Hautière, J.-P. Tarel, and D. Aubert, “Mitigation of visibility loss for advanced camera based driver assistances,” *Trans. on Intelligent Transportation Systems*, vol. 11, no. 2, pp. 474–484, 2010.
- [6] L. Rudin, S. Osher, and E. Fatemi, “Nonlinear total variation based noise removal algorithms,” *Physica. D*, vol. 60, pp. 259–268, 1992.
- [7] J.-P. Tarel, N. Hautière, A. Cord, D. Gruyer, and H. Halmoui, “Improved visibility of road scene images under heterogeneous fog,” in *IEEE Intelligent Vehicles Symposium*, 2010.
- [8] Y. Zhang, B. Guindon, and J. Cihlar, “An image transform to characterize and compensate for spatial variations in thin cloud contamination of landsat images,” *Remote Sensing of Environment*, vol. 82, no. 2, pp. 173–187, 2002.
- [9] N. Hautière, J.-P. Tarel, J. Lavenant, and D. Aubert, “Automatic fog detection and estimation of visibility distance through use of an onboard camera,” *Machine Vision and Applications*, vol. 17, no. 1, pp. 8–20, 2006.



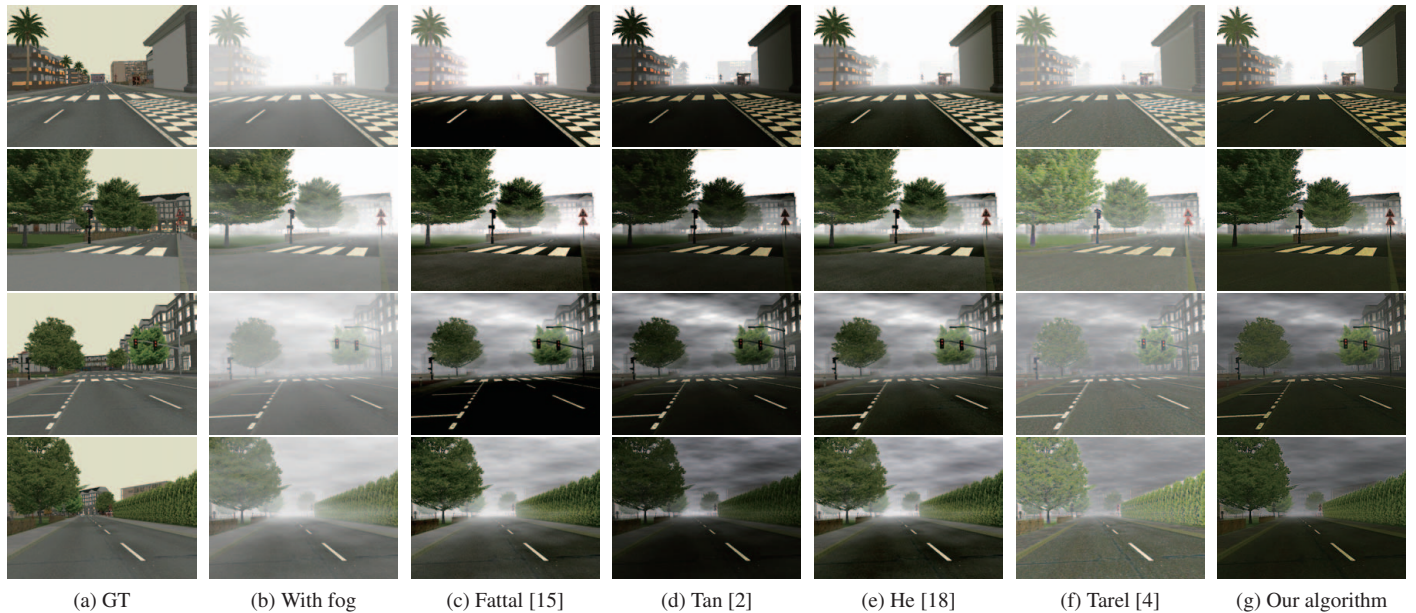


**Fig. 6.** Sample results of quantitative evaluation of our algorithm on the synthetic scenes generated by [5]. (a) The image without fog. (b) The hazy image. (c)-(e) The results obtained by Fattal [15], Tan [2], He et al. [18], Tarel et al.[4] and our algorithm. 1<sup>st</sup> row: scene sample with uniform fog. 2<sup>nd</sup> row: scene sample with heterogeneous  $k$  fog. 3<sup>rd</sup> row: scene sample with heterogeneous  $L_\infty$  fog. 4<sup>th</sup> row: scene sample with heterogeneous  $k$  and  $L_\infty$  fog.

- [10] N. Hautière and D. Aubert, “Contrast restoration of foggy images through use of an onboard camera,” in *IEEE Trans. on Intelligent Transportation Systems*, 2005, pp. 601–606.
- [11] Y. Schechner, S. Narasimhan, and S. Nayar, “Instant dehazing of images using polarization,” in *CVPR*, 2001.
- [12] S. Narasimhan and S. Nayar, “Interactive deweathering of an image using physical models,” in *IEEE Workshop on Color and Photometric Methods in Computer Vision*, 2003.
- [13] L. Schaul, C. Fredembach, and S. Süsstrunk, “Color image dehazing using the near-infrared,” in *ICIP*, 2009.
- [14] J. Kopf, B. Neubert, B. Chen, M. Cohen, D. Cohen-Or, O. Deussen, M. Uyttendaele, and D. Lischinski, “Deep photo: Model-based photograph enhancement and viewing,” *ACM Trans. on Graphics*, vol. 27, no. 5, 2008.
- [15] R. Fattal, “Single image dehazing,” *ACM Transaction on Graphics*, vol. 27, no. 3, pp. 1–9, 2008.
- [16] J. Zhang, L. Li, G. Yang, and Y. Zhang, “Local albedo-insensitive single image dehazing,” *The Visual Computer*, vol. 26, no. 6-8, pp. 761–768, 2010.
- [17] E. Matlin and P. Milanfar, “Removal of haze and noise from a single image,” in *SPIE Conference on Computational Imaging*, 2012.
- [18] K. He, J. Sun, and X. Tang, “Single image haze removal using dark channel prior,” in *CVPR*, 2009.
- [19] K. He, J. Sun, and X. Tang, “Guided image filtering,” in *ECCV*, 2010.
- [20] L. Kratz and K. Nishino, “Factorizing scene albedo and depth from a single foggy image,” in *ICCV*, 2009.
- [21] N. Hautière, J.-P. Tarel, D. Aubert, and E. Dumont, “Blind contrast enhancement assessment by gradient ratioing at visible edges,” *Image Analysis & Stereology Journal*, vol. 27, no. 2, pp. 87–95, 2008.
- [22] A. Chambolle, V. Caselles, M. Novaga, D. Cremers, and T. Pock., “An introduction to total variation for image analysis,” <http://hal.archives-ouvertes.fr/docs/00/43/75/81/PDF/preprint.pdf>, 2009.
- [23] A. Chambolle, “Total variation minimization and a class of binary mrf models,” in *EMMCVPR*, 2005.
- [24] Liang Li, Wei Feng, Liang Wan, and Jiawan Zhang, “Maximum cohesive grid of superpixels for fast object localization,” in *CVPR*, 2013.